where we used the change of variable $x' = x + (\lambda - R_s)t$ to obtain the second term. Evaluating the above integrals we have

$$\begin{aligned} F_s(\theta) &= \frac{1}{\theta q_s(q_s - \theta(\lambda - R_s))}\left[e^{-\theta B_1} q_s - e^{-\theta B_2}(q_s - \theta(\lambda - R_s)(1 - e^{-\frac{q_s}{R_s - \lambda}(B_2 - B_1)}))\right] \\ &+ \frac{1}{q_s - \theta(\lambda - R_s)} \sum_{s' \neq s} q_{ss'} \left[F_{s'}(\theta) - e^{-(\theta - \frac{q_s}{\lambda - R_s})B_2} F_{s'}\left(\frac{q_s}{\lambda - R_s}\right)\right] \end{aligned} \tag{19}$$

Comparing (18) and (19) we observe that both equations have the same form with B_1 and B_2 interchanged. Multiplying both sides of (18) and (19) with $q_s - \theta(\lambda - R_s)$ and arranging the terms, we obtain the matrix equation

$$(Q + \theta D)\underline{F}(\theta) = \underline{b}(\theta)$$

where $\underline{b}(\theta) = [b_1(\theta), \ldots, b_N(\theta)]^T$ is given by

$$\begin{aligned} b_s(\theta) &= \frac{1}{\theta q_s}\left[-e^{-\theta B_1}(q_s - \theta(\lambda - R_s)(1 - e^{-\frac{q_s}{\lambda - R_s}(B_2 - B_1)})) + e^{-\theta B_2} q_s\right] \\ &+ e^{-(\theta - \frac{q_s}{\lambda - R_s})B_1} \sum_{s' \neq s} q_{ss'} F_{s'}\left(\frac{q_s}{\lambda - R_s}\right) \end{aligned} \tag{20}$$

for a state s with $\lambda > R_s$. For s with $\lambda < R_s$, $b_s(\theta)$ is same as (20) with B_1 and B_2 interchanged. $b_s(\theta)$ contains $N(N-1)$ unknown constants $\{F_{s'}\left(\frac{q_s}{\lambda - R_s}\right)\}_{s \neq s'}$.

These constants correspond to the discontinuity of $E[\tau|s, x]$ at B_1 or B_2. For a state s with $\lambda > R_s$

$$\lim_{x \nearrow B_2} E[\tau|s, x] = 0$$

whereas

$$\lim_{x \searrow B_1} E[\tau|s, x] > 0$$

although $E[\tau|s, B_1] = 0$. Similarly, for a state s with $\lambda < R_s$, the discontinuity occurs at B_2. We can write for s with $\lambda > R_s$

$$b_s(\theta) = -\frac{1}{\theta}(e^{-\theta B_1} - e^{-\theta B_2}) + \gamma_s e^{-\theta B_1} \tag{21}$$

and for a state s with $\lambda < R_s$,

$$b_s(\theta) = -\frac{1}{\theta}(e^{-\theta B_1} - e^{-\theta B_2}) + \gamma_s e^{-\theta B_2} \tag{22}$$

where the unknown constants $\{\gamma_s\}$ can be expressed from (20). These constants will be evaluated by taking the inverse Laplace transform of $\underline{F}(\theta) = (Q + \theta D)^{-1}\underline{b}(\theta)$ and applying the boundary conditions: For each state s with $\lambda > R_s$, we set $E[\tau|s, B_2] = 0$ and for s with $\lambda < R_s$, we set $E[\tau|s, B_1] = 0$. Since $\{\gamma_s\}$ appear as coefficients in the corresponding mean passage time equations, $\{\gamma_s\}$ can be obtained as the solution of a system of N linear equations.

Appendix A: Derivation of $\underline{F}(\theta)$

In this part we derive the Laplace transform $F_s(\theta)$ of $E[\tau|s,x]$ with respect to x and show that the N-dimensional vector $\underline{F}(\theta)$ given by (4) can be represented by (5).

Case 1: $\lambda > R_s$

Taking the Laplace transform of (1), we have

$$\begin{aligned} F_s(\theta) &= \int_{B_1}^{B_2} e^{-\theta x} e^{-q_s \frac{B_2-x}{\lambda-R_s}} \frac{B_2-x}{\lambda-R_s} dx \\ &\quad + \sum_{s' \neq s} q_{ss'} \int_{B_1}^{B_2} e^{-\theta x} \int_0^{\frac{B_2-x}{\lambda-R_s}} e^{-q_s t} [t + E[\tau|s', x+(\lambda-R_s)t]] dt dx \\ &= \frac{1}{q_s} \int_{B_1}^{B_2} e^{-\theta x} (1 - e^{-q_s \frac{B_2-x}{\lambda-R_s}}) dx \\ &\quad + \sum_{s' \neq s} q_{ss'} \int_{B_1}^{B_2} e^{-\theta x'} E[\tau|s', x'] \int_0^{\frac{x'-B_1}{\lambda-R_s}} e^{-(q_s - \theta(\lambda-R_s))t} dt dx' \end{aligned}$$

where we used the change of variable $x' = x + (\lambda - R_s)t$ to obtain the second term.

$$\begin{aligned} F_s(\theta) &= \frac{1}{q_s} \left[\frac{1}{\theta} (e^{-\theta B_1} - e^{-\theta B_2}) + \frac{(\lambda-R_s) e^{\frac{-q_s B_2}{\lambda-R_s}}}{q_s - \theta(\lambda-R_s)} \left(e^{-(\theta - \frac{q_s}{\lambda-R_s})B_1} - e^{-(\theta - \frac{q_s}{\lambda-R_s})B_2} \right) \right] \\ &\quad + \frac{1}{q_s - \theta(\lambda-R_s)} \sum_{s' \neq s} q_{ss'} \left[F_{s'}(\theta) - e^{-(\theta - \frac{q_s}{\lambda-R_s})B_1} \int_{B_1}^{B_2} E[\tau|s', x'] e^{-\frac{q_s}{\lambda-R_s} x'} dx' \right] \\ &= \frac{1}{\theta q_s (q_s - \theta(\lambda-R_s))} \left[e^{-\theta B_1} (q_s - \theta(\lambda-R_s)(1 - e^{-\frac{q_s}{\lambda-R_s}(B_2-B_1)})) - e^{-\theta B_2} q_s \right] \\ &\quad + \frac{1}{q_s - \theta(\lambda-R_s)} \sum_{s' \neq s} q_{ss'} \left[F_{s'}(\theta) - e^{-(\theta - \frac{q_s}{\lambda-R_s})B_1} F_{s'} \left(\frac{q_s}{\lambda-R_s} \right) \right] \end{aligned} \tag{18}$$

Case 2: $\lambda < R_s$

Taking the Laplace transform of (2), we have

$$\begin{aligned} F_s(\theta) &= \int_{B_1}^{B_2} e^{-\theta x} e^{-q_s \frac{x-B_1}{R_s-\lambda}} \frac{x-B_1}{R_s-\lambda} dx \\ &\quad + \sum_{s' \neq s} q_{ss'} \int_{B_1}^{B_2} e^{-\theta x} \int_0^{\frac{x-B_1}{R_s-\lambda}} e^{-q_s t} [t + E[\tau|s', x+(\lambda-R_s)t]] dt dx \\ &= \frac{1}{q_s} \int_{B_1}^{B_2} e^{-\theta x} (1 - e^{-q_s \frac{x-B_1}{R_s-\lambda}}) dx \\ &\quad + \sum_{s' \neq s} q_{ss'} \int_{B_1}^{B_2} e^{-\theta x'} E[\tau|s', x'] \int_0^{\frac{B_2-x'}{R_s-\lambda}} e^{-(q_s - \theta(\lambda-R_s))t} dt dx' \end{aligned}$$

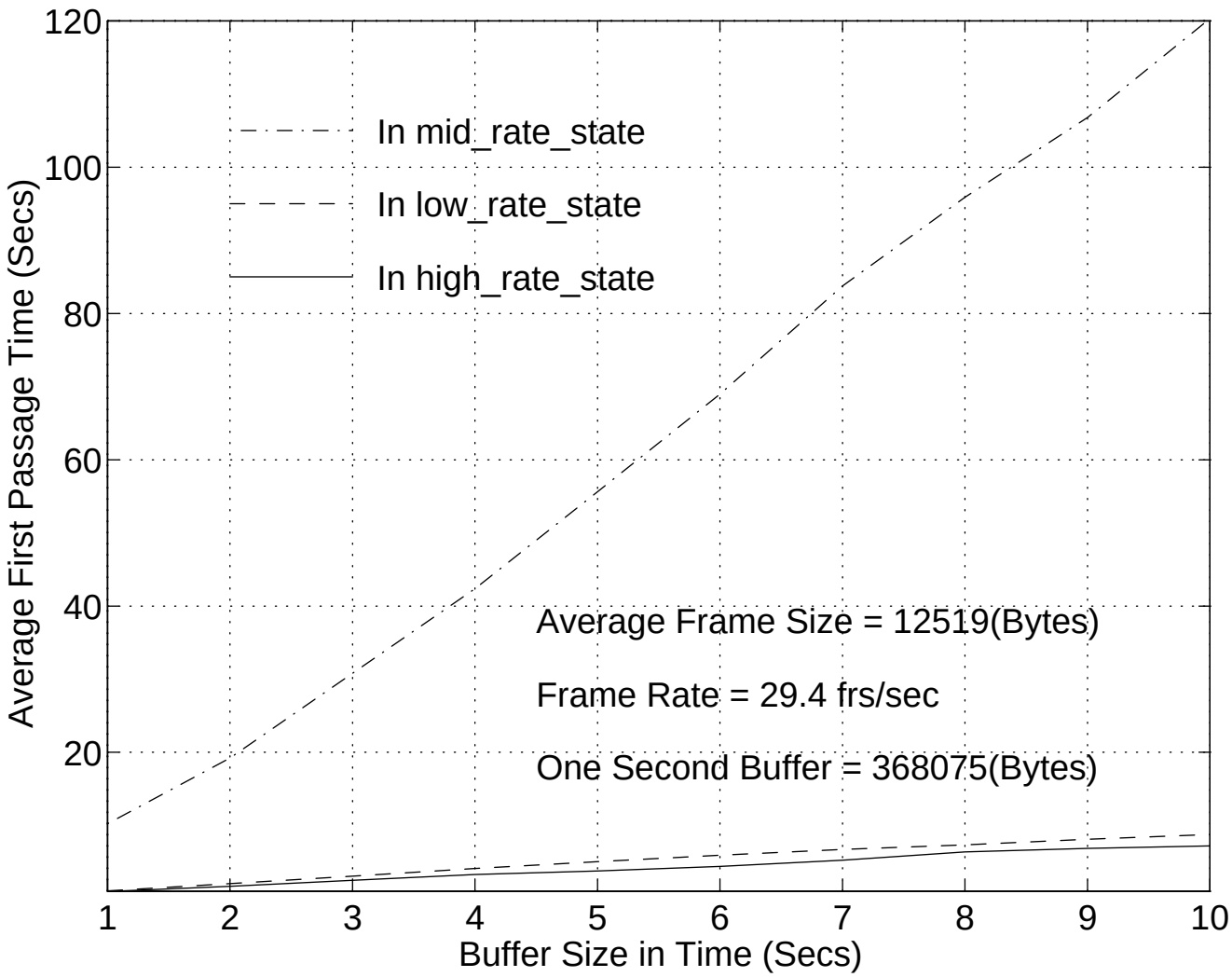

Figure 13: First passage times relative to buffer size

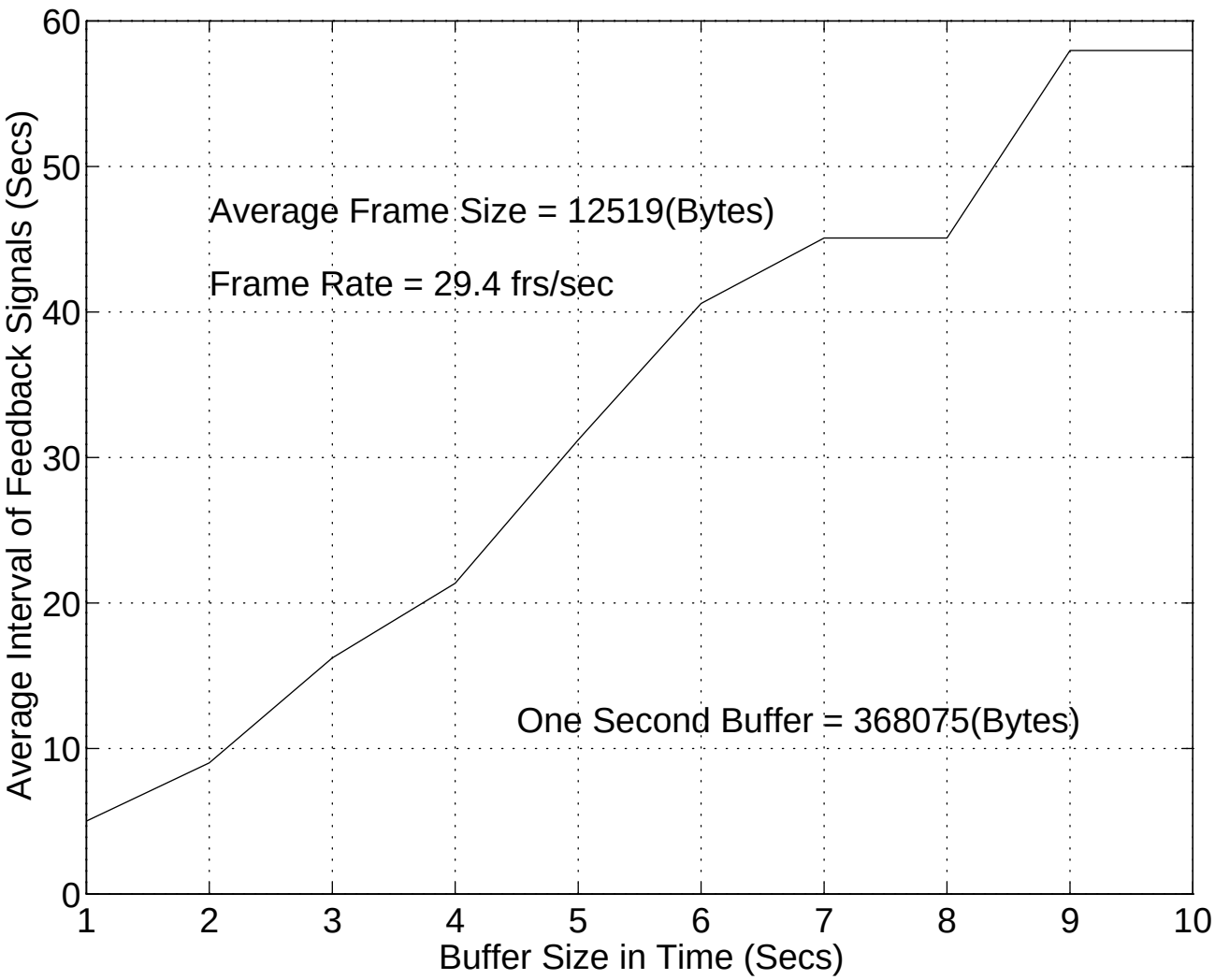

Figure 12: Signaling frequencies relative to buffer size

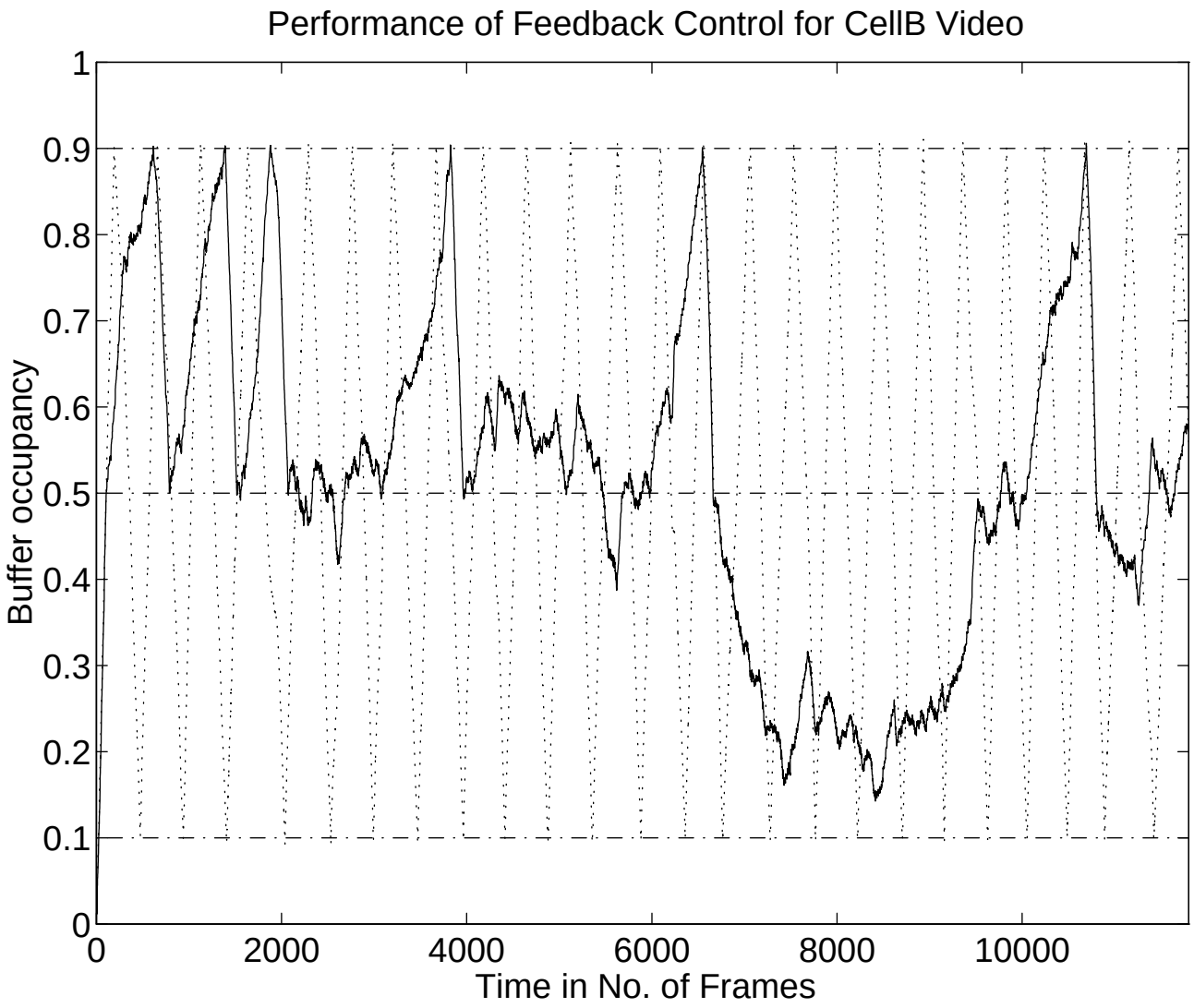

Figure 11: Buffer occupancy variation for the CellB video

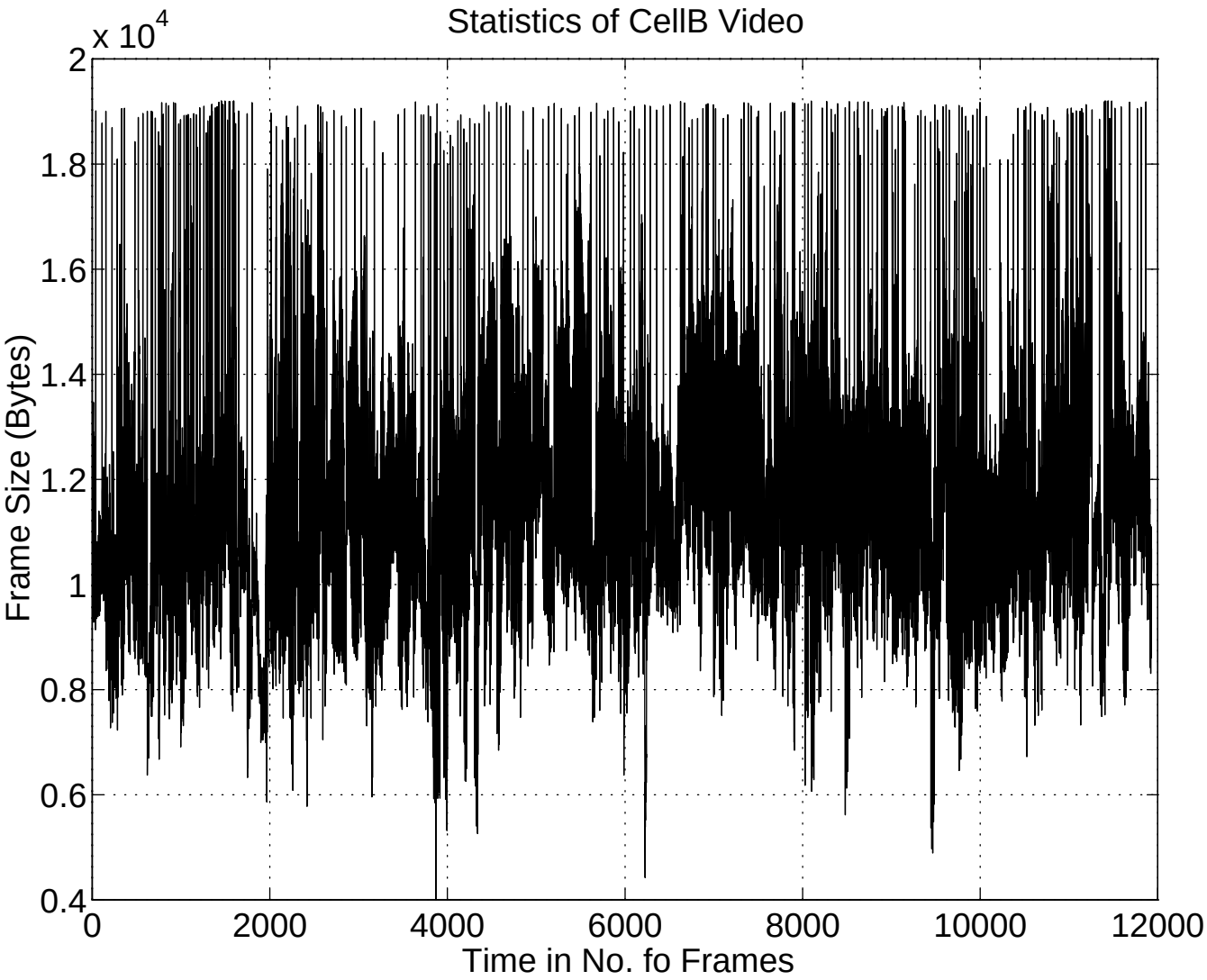

Figure 10: A CELLB video sequence

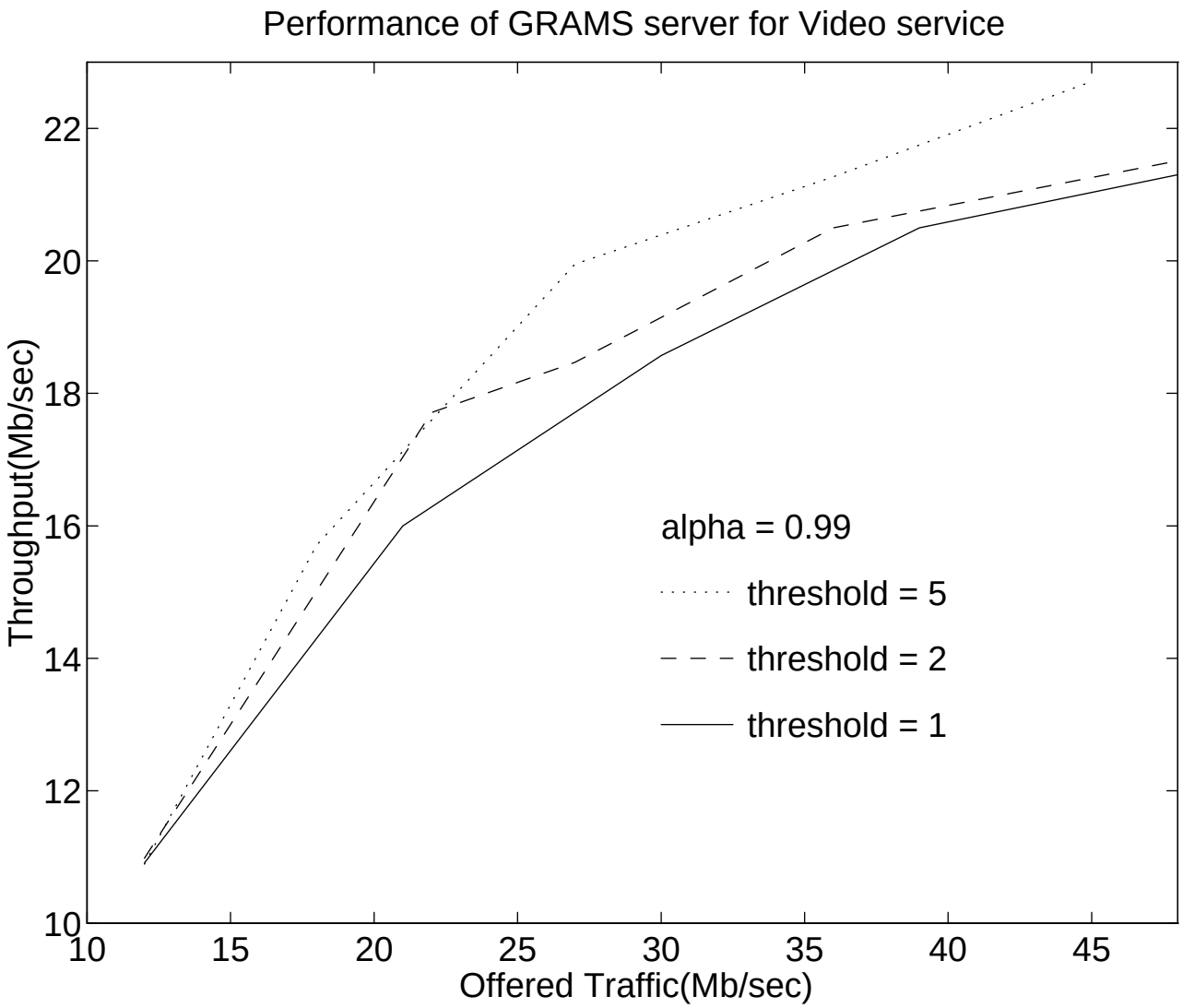

Figure 9: Server throughput

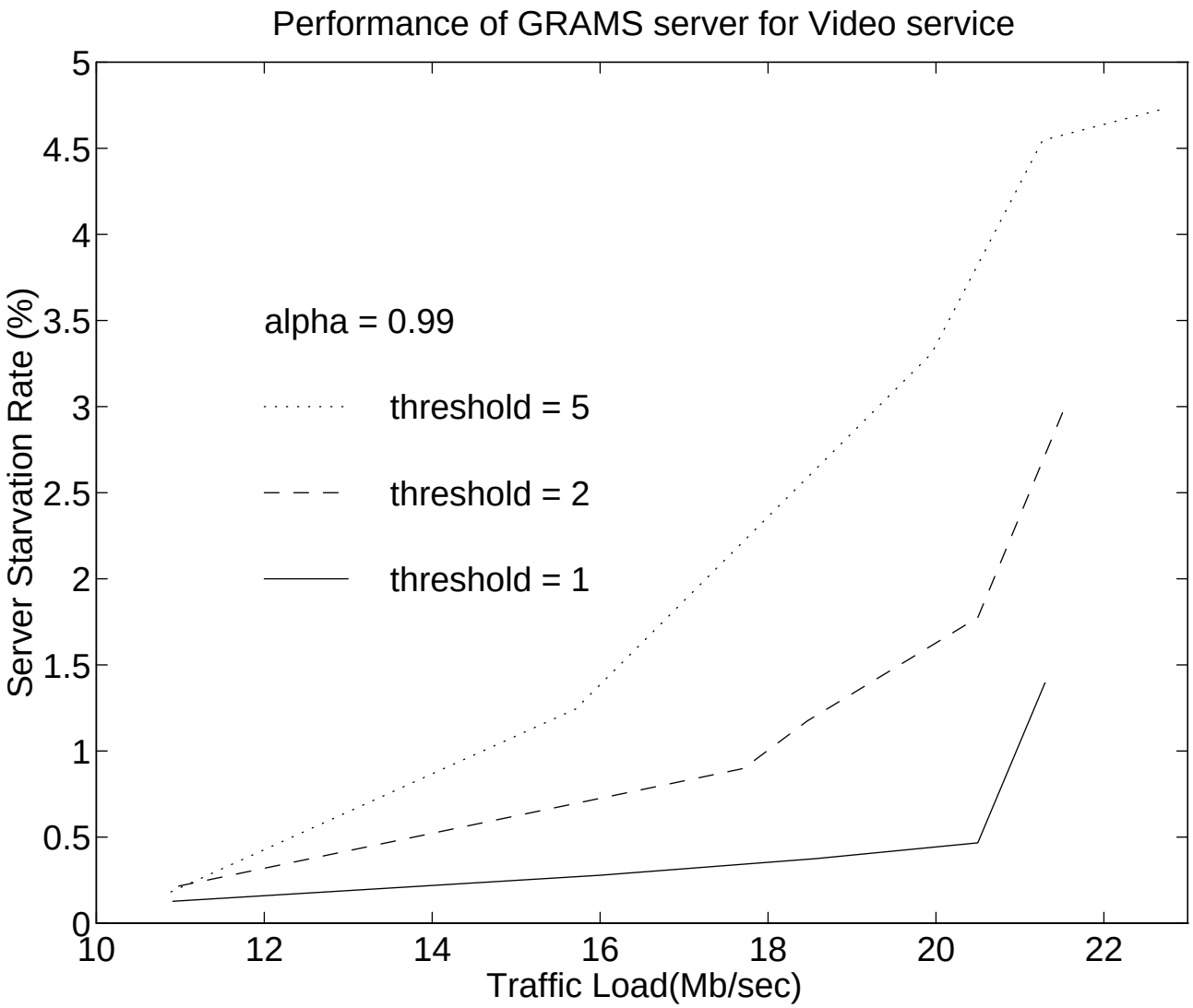

Figure 8: Server starvation rate

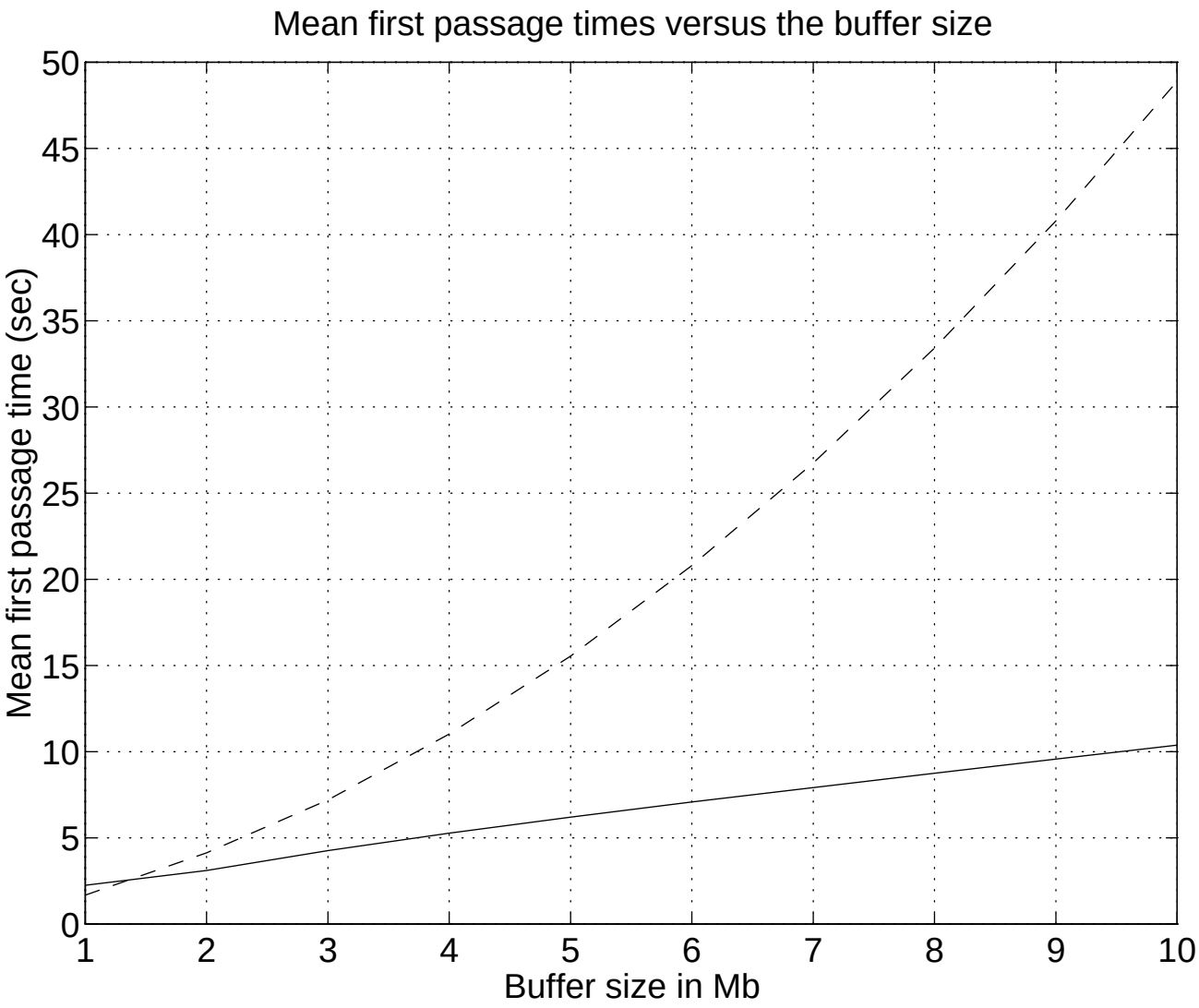

Figure 7: Mean first passage times as a funtion of buffer size

References

[1] Joseph Hui, Junbiao Zhang, Jun Li: "Quality of Service control in GRAMS for ATM Local Area Network", To appear in *IEEE Journal of Selected Areas in Communications*

[2] Joseph Hui: "Resource Allocation for Broadband Networks", IEEE Journal on Selected Areas in Communications, Vol. 6, No. 9, December 1988.

[3] D. Reininger, B. Melamed, D. Raychaudhuri, "Variable Bit Rate MPEG video: Characteristics, Modeling and Multiplexing," in Proceedings of the 14th Internation Teletraffic Congress, Antibes Juan-les-Pins, France, 6-10 June, 1994.

[4] Deniel Minoli, Robert Keinath: "Distributed Multimedia Through Broadband Communications Services", 1994 Artech House, Inc.

[5] SunSoft Incorporated: "CellB Codec", Imaging Library Programmer's Guide(Solaris XIL 1.1 Imaging Library AnswerBook).

[6] P.Vendat Rangan and Harrick M. Vin: "Designing an On-Demand Multimedia Service", IEEE Communications Magazine, Vol. 30, No. 7, July 1992, pp. 56-65

[7] T.D.C. Little and F. Kao: "An Intermedia Skew Control System for Multimedia Data Presentation", Proc. 3rd International Workshop on Network and Operating System Support for Digital Audio and Video , La Jolla, CA, November 1992, pp. 121-132.

[8] A. Pitsillides and J. Lambert: "Adaptive connection admission and flow control: Quality of service with high utilisation", in Proceedings of the Conference on Computer Communications (IEEE Infocom), (Toronto, Canada), June 1994.

[9] G. Ramamurthy and R. S. Dighe, "Distributed source control: a network access control for integrated broadband packet networks," IEEE Journal on Selected Areas in Communications, vol. 9, pp. 990–1002, Sept. 1991

[10] William Stallings: *Advances in ISDN and Broadband ISDN*, IEEE Computer Society Press

[11] D. Anick, D. Mitra and M. M. Sondhi, "Stochastic Theory of Data-Handling Systems with Multiple Sources," Bell System Technical Journal, Vol. 61, No. 8, Oct. 1982, pp. 1871-1893.

[12] Howard P. Katseff and Bethany S. Robinson: " Predictive Prefetch in the Nemesis Multimedia Information Service", ACM Multimedia '94, October, San Francisco

[13] F. Anklesaria: "F.Y.I on the Internet Gopher Protocol(a distributed document search" and retrieval protocol)", available from gopher://gopher.micro.umn.edu

[14] Nathan Torkington: "World Wide Web Primer": available from http://www.vuw.ac.nz/non-local/gnat/www-primer.html

[15] NCSA Software Development Group: "NCSA Mosaic Documentation", available from http://www.ncsa.uiuc.edu/SDG/Software/Mosaic/Docs/mosaic-docs.html

[16] Rob McCool(NCSA Software Development Group): "NCSA httpd Overview", available from http://hoohoo.ncsa.uiuc.edu/docs/Overview.html

$$\text{High rate } \lambda_h = 1.5 * R_b$$

$$\text{Medium rate } \lambda_m = R_b$$

$$\text{Low rate } \lambda_l = 0.5 * R_b$$

where T ranges from 1 second to 10 seconds in our tests.

Figure 11 demonstrates a typical buffer occupancy change as the client consumes the video stream obtained from the GRAMS server. $T = 5$ *seconds* in this test. The curve in solid line shows the occupancy variations based on the feedback mechanism described earlier. The curve in dashed line gives the result when the medium threshold T_m is not used(i.e. the server only transmits at either the high rate λ_h or the low rate λ_l in response to client signals). In both cases, no buffer underflow or overflow occurs. We observe that the high threshold and low threshold are reached much less frequently when the medium threshold is set for the buffer. This will lead to a lower probability of buffer underflowing and overflowing. Rate changes are also reduced in this case.

Figure 12 shows the change of average time interval between two consecutive feedback signals as the buffer size increases. Even if we only use a buffer size corresponding to 1 second video stream, the interval is still bigger than 5 seconds. Therefore, the overhead of feedback signaling is very small.

Figure 13 shows the first passage times of the three transmit states. As explained in section 3, we distinguish three states according to the transmission rates the server chooses. The first passage time of each state denotes the average duration in which the server uses the corresponding rate. The curves show certain similarities to those in figure 7 which is from the two state Markov model. However, the first passage time of medium rate state exhibits more linearity than exponetiality. Therefore, the ratio of the server using midium rate to low/high rate is almost unchanged with respect to the buffer size. The server spends about 4 times longer in the medium rate state than in the low/high rate states.

These test results show the adaptiveness of the feedback mechanism in accommodating the fluctuations. The intuitive choices for the values of the thresholds and the rates are justified by the relatively smooth changes of the buffer occupancy and the transmit rates.

5. Conclusions

We have demonstrated the adaptiveness and efficiency of client-based rate and synchronization control through the GRAMS implementation. Currently, we are refining the interface and performing further traffic studies based on real applications. Also, we presented new performance analysis methodologies using first passage time analysis, for which both the state of the buffer and the state of the video encoding algorithm are considered.

The current GRAMS server as well as the client interface and control are functioning as expected in our current implementation. Further experience will be gained and reported as the server and client will be deployed locally on our campus.

client to perform simple book keeping to keep track of which audio-video groups have arrived in full without errors. Only those groups (or one half of a group) without errors will be displayed. However, since the quality of the audio is of paramount importance, every attempt is made to conserve and play back the received audio. The packet header contains the byte address (with respect to the beginning of the audio-video file) of the first byte of data in the packet, as well the number of bytes of data in the packet.

Finally, we present experimental traffic statistics as a result of client feedback based on receive buffer occupancy. The result is based on the video coding method CELLB, which is the currently available variable rate video encoding algorithm on our computing platform. The experiment is performed on a video stream for which a typical trajectory of the encoded size of frames is shown in figure 10. The video stream has the following statistics:

Frame number N = 12000

Frame rate R_f = 29.4 fps

Bit rate R_b = 334414 Bps

Statistics and modeling of variable rate MPEG can be found in [3]. Since we employ multiple audio-video standards as well as multiple sub-sampled frame rates, it seems from these rate trajectories that a proper modeling and adaptation of the model as a function of control could be quite complex. Our control approach is highly adaptive and does not require traffic statistics to be known a priori other than the average rate (for the full rate and perhaps for the sub-sampled rate). Nevertheless, it is helpful to obtain traffic statistics of the requested rates by the client for the following purposes:

- Bandwidth engineering such as the sizing of bandwidth for a virtual path.
- Estimating the amount of signaling required due to these requests.
- Sizing the client buffer in order to maintain good QoS.

The choices of buffer size and thresholds affect the feedback frequency which indicates the overhead incurred by signaling and rate changes. Determining a proper combination of buffer size, thresholds and the corresponding transmission rates for a specific stream is much complicated due to too many changing factors. In order to avoid overwhelming complexities, make the three thresholds proportional to the buffer size and the three rates proportional to the average rate of the video stream. Tests are then made to find out the buffer occupancy changes with respect to different buffer sizes. The actual values of the parameters are as follows:

Buffer size $S = T * R_b$

High Threshold $T_h = 0.9 * S$

Medium Threshold $T_m = 0.5 * S$

Low threshold $T_l = 0.1 * S$

besides I and P frames.) The number of frames in a group was chosen so that we may restart from an I frame should packet loss or error occur during transmission within the group, or from an I frame of the next group. Also, the grouping allows scaling back of the video rate if the network is found to be a bandwidth bottleneck(Figure 6).

In a separate pointer file, we store headers for each audio-video group. The header makes it easy for the server to find the I frames if for some reason it needs to decimate the video stream by dropping frames. The header contains the offset of the beginning and the end of the first and third frames, which are I frames for both motion JPEG and MPEG. The audio part precedes the the location indicated by the offset of the first frame. These offsets are transmitted as the header for the group which are used both by the server and the client during media transmission and playback.

Two features complicate the design of the audio-video synchronization scheme: media scalability and transport protocol support. These two features handles problems resulting from network bandwidth bottleneck, packet loss, and server/client overload.

As discussed earlier, the client detects network congestion and requests a downward scaling of the media to relieve the bandwidth bottleneck. Our grouping would allow frame rates of 30 frames per second, 10 frames per second (by transmitting the audio plus first and third I frames only), 5 frames per second (by transmitting the audio plus the first I frames), 2.5 frames per second (by transmitting the audio for every group and the video every other group), as well as lower rates such as 1 frame per second, every two seconds, every 5 seconds, etc. The downward adjustment is automatic until the requested transmission rate matches the receive rate. Upward frame rate adjustment is initiated by the end-user through a control on the client interface. We note also that caching is performed for the maximum frame rate even though only part of the cached media may be transmitted. It is not difficult to cache only the transmitted information, but the increased disk seek time and address computations may outweigh the advantages of decreased disk reading time and reduced cache size.

The transmitter may employ transport protocol such as TCP or UDP. Since image transport typically requires almost no packet loss and we may tolerate one or more seconds of image transport latency, using TCP as a transport mechanism could be appropriate. For audio-video applications, TCP may incur unnecessary retransmission, delay, and processing. One option for audio-video transport is to add minimal transport layer functions within the application for packets piped via ATM and AAL 4/5[10].

To handle out-of-order packets and packet loss, additional information is inserted into the packet header. For audio-video applications, packet loss may result in discarded or repeated audio-video segments, and currently, we do not attempt to retransmit lost packets to avoid retransmission delay and additional complexity in caching, retransmission scheduling, and preventing packet duplication. As described earlier, rate control is exercised by packet size assignment. Since most networks impose a maximum packet size (e.g. 4 kilobytes), several packets will be needed to transport one audio-video group. In GRAMS, each audio-video group will be transported by an integer number of packets so that each packet may contain information of two different groups. This allows the

by actions such as reducing the packet size for images. Admission control delays new admissions until the QoS parameter recedes. Figure 8 plots the overall system starvation rate as a function of the offered load, α, and thresholds for video. As expected, starvation increases as offered load is increased. Starvation can occur even at low load because of rather unpredictable load in each round for the operating system, making available processing cycles in each round for caching and transmission functions somewhat unpredictable. Such starvation has the effect of gating admission very much the same way as a traffic light. Figure 9 plots the carried load as a function of the offered load (assuming failed admission are cleared instead of being queued). The difference between carried load and the offered load reflects the fraction of connection requests which suffers delay (often minimal) before the connection is completed. Thus, we have a system that is adaptive and degrades gracefully as system load is increased, and requires very little knowledge of traffic statistics.

Next, we focus on media scaling and synchronization between the different media in GRAMS. In GRAMS, a typical application is stored lectures which often involves the synchronization of the video (e.g. the lecture scene), audio (e.g. the lecturer's speech which often carries most of the cognitive information of the lecture), and image streams (e.g. lecture transparencies). We call this an audio-video-visual session. The audio-video synchronization requirement is very stringent with a discrepancy of less than 100 milliseconds, whereas the video-image synchronization requirement could be quite loose with an allowable discrepancy of seconds. Therefore, the media synchronization discussed here will be primarily between the video and audio streams.

There are two components of audio-video synchronization. First, maintain the natural rate of playback of audio, which from a subjective point of view is more important than the natural rate of playback of video[12]. Hence, we shall maintain the continuity of the audio, at the expense of possibly more jitter for the video. Second, we need to synchronize the audio stream with the video stream for obvious qualities such as "lip synchronization", etc.

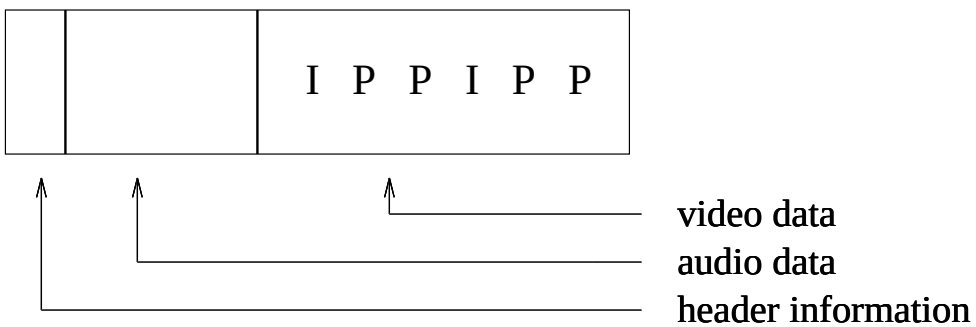

Figure 6: Structure of the video-audio block

Many currently available technologies record and store the audio and video streams separately. This complicates the synchronization of the two media. In the GRAMS experiments, we group the streams into audio/video groups. Each audio/video group consists of six frames of video preceded by the audio data of the group. We assume the natural frame rate of 30 frames per second. For our current implementation, we use three video formats: motion JPEG which consists of I frames, MPEG which consists of periodic IPP frames, or CELLB. (The MPEG standard contains B frames

Quick response data This includes images, postscript files for transparencies, etc. for which the major QoS concern is latency.

Time insensitive data This includes all sorts of retrieval data which do not have strict delay requirements.

The service of these three queues is done in a round robin fashion in rounds of fixed duration(Figure 5). A packet is sent for each connection in a round. The rate of the connection is therefore given by the packet size divided by the duration of the round. Rate assignment is done by packet size assignment during connection setup. Rate adjustment by changing the packet size occurs when feedback requests are made downstream by the client. The packets are served according to the priority of the media type described above. Transmission starvation (or jitter) occurs for a connection when a packet for that connection is not transmitted within that round. Cache starvation occurs when a packet cannot be transmitted in a round due to cache underflow.

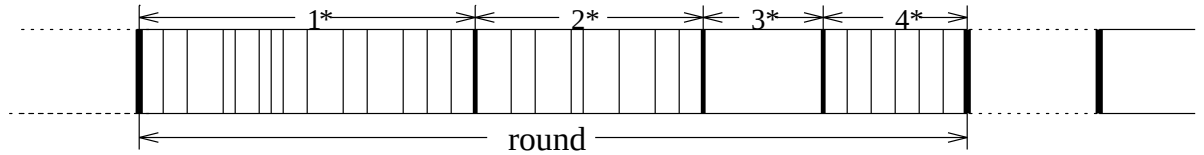

1*: Schedule continuous real-time requests

2*: Schedule quick-response requests

3*: Check to accept new connection requests

4*: Schedule retrieval purpose requests

Figure 5: Basic frame structure

We monitor the QoS at the server by computing the underflow jitter rate of the transmit value. The starvation count is updated per round for each connection i according to

$$C_i \leftarrow \alpha_i C_i + I_i \tag{17}$$

in which $I_i = 1$ if during the round, no packet is sent due to cache underflow or transmission starvation. Compensation of transmission may occur if the round has time left over and if C_i is positive. In this case, I_i is equal to one minus the number of packets transmitted for the connection i. For quick response data services such as image transport, we set $\alpha_i = 1$ so that C_i represents the cumulative transmission deficit. For video transmission, we set $\alpha_i < 1$ so that C_i represents a geometrically weighted running sum of the transmission deficit.

The single parameter C_i keeps track of the QoS for which the server is trying to maintain for the connection i. However, the actual QoS perceived by the client is better than C_i because further buffering and smoothing of jitter is performed at the client. Nevertheless, the local server QoS parameter is useful because the degradation of this QoS parameter can result from usage congestion of any resource such as the disk bus, cache memory, transmission bandwidth, or processing cycles. When the parameter exceeds a certain threshold, GRAMS attempts to reduce usage congestion by exercising rate control and admission control. Rate control reduces the rates of quick response data

The thresholds T_l, T_m and T_h are chosen as

$$T_l = 0.1B_M, \;\; T_m = 0.5B_M \text{ and } T_h = 0.9B_M$$

and B_M varies from $1Mbs$ to $10Mbs$ (1 second to 10 seconds of video). The mean first passage times are shown in Figure 7 as a function of buffer size, where the solid curve represents $E[\tau_1] = E[\tau_2]$ and the dashed curve corresponds to $E[\tau_3]$.

When B_M is large $E[\tau_1]$ and $E[\tau_2]$ are dominated by the first term in (13) and (14) respectively. The reason for this is as B_M gets larger, the mean first passage times also increase and the effect of the initial state is washed out.

When the transmission rate is λ_m, the average drift is zero. $E[\tau_3]$ is determined by the occurrence of a temporary overload or underload period whose duration should increase as B_M gets larger. Since the time spent at each state is exponentially distributed, the probability of a long enough overload or underload period decreases exponentially as B_M increases. Therefore, $E[\tau_3]$ increases exponentially with the buffer size. For large enough buffer size, starting at the medium threshold, the mean time to hit the lower or upper threholds is quite large and the buffer length will rather quickly return to the medium threshold after hitting either lower or upper thresholds.

4. Implementation of Multimedia Server and Client Interface

In addition to the multimedia server GRAMS[1], we implemented a client interface which provides client-based synchronization and QoS control via feedback. This section describes the issues for the implementation of both the server and the client.

GRAMS (Gopher-style Real-time ATM Multimedia System) is a distributed multimedia system which can be deployed on an ATM LAN, a wide area ATM network, or the Internet environment. The most noticeable features of this system are:

- GRAMS is fully compatible with several popular Internet document retrieval protocols including gopher[13] and http[16]. The client interface of GRAMS employs the popular media viewer Mosaic[15], which provides integrated multimedia display as well as the World-Wide Web Navigation help[14].
- The GRAMS server can provide heterogeneous media services such as video, audio, image, and text with Quality of Service (QoS) control.
- Several video formats (including MPEG , motion JPEG[4]and CELLB[5]) are supported in addition to image formats such as JPEG and GIF.
- GRAMS supports multiple transport protocols include TCP, UDP and ATM with AAL4[10].

In GRAMS, three types of media are distinguished and a queue is associated with each media type. In decreasing order of service priority, they are:

Continuous real-time media This includes video (CBR and VBR video) and audio which require continuous transmission and playback. The major QoS concerns are latency and jitter as defined earlier.

We find the mean values of τ_1, τ_2 and τ_3 separately.

A. $E[\tau_1]$:

Since $R_1 < \lambda_m < R_2$, the chain is in state 1 when T_h is hit, i.e., $E[\tau_1] = E[\tau_1|1]$. By doing the partial fraction expansion in (7) and taking the inverse Laplace transform with respect to θ, with $Re\{\theta\} > 0$, we obtain

$$E[\tau_1] = -\frac{(\alpha+\beta)(T_h - T_m)}{\beta(\lambda_l - R_1) + \alpha(\lambda_l - R_2)} + \frac{\alpha(R_1 - R_2)(\lambda_l - R_2)}{[\beta(\lambda_l - R_1) + \alpha(\lambda_l - R_2)]^2}(1 - e^{\theta_1(\lambda_l)(T_h - T_m)}) \tag{13}$$

The first term in (13) corresponds to the steady state behavior of the Markov chain, whereas the second term reflects the effect of the initial state.

B. $E[\tau_2]$:

Since $R_1 < \lambda_m < R_2$, the chain is in state 2 when T_l is hit, i.e., $E[\tau_2] = E[\tau_2|2]$. By doing the partial fraction expansion in (7) and taking the inverse Laplace transform with respect to θ, with $Re\{\theta\} < 0$, we obtain

$$E[\tau_2] = \frac{(\alpha+\beta)(T_m - T_l)}{\beta(\lambda_h - R_1) + \alpha(\lambda_h - R_2)} + \frac{\beta(R_2 - R_1)(\lambda_h - R_1)}{[\beta(\lambda_h - R_1) + \alpha(\lambda_h - R_2)]^2}(1 - e^{\theta_1(\lambda_h)(T_l - T_m)}) \tag{14}$$

C. $E[\tau_3]$:

The state of the chain at the beginning can be either 1 or 2. Since $R_1 < \lambda_m < R_2$, we need to evaluate the boundary conditions. Solving the linear system of equations we obtain the two unknown constants:

$$\gamma_1 = \frac{(\alpha+\beta)(T_h - T_l)^2/2 - (\lambda_m - R_2)(T_h - T_l)}{\beta(T_h - T_l) - (\lambda_m - R_2)}$$

$$\gamma_2 = \frac{(\alpha+\beta)(T_h - T_l)^2/2 - (\lambda_m - R_1)(T_h - T_l)}{\lambda_m - R_1 - \alpha(T_h - T_l)}$$

Performing the partial fraction expansion and taking the inverse Laplace transform we obtain

$$E[\tau_3|1] = \frac{(\lambda_m - R_2)\gamma_1 - (\beta\gamma_1 + \lambda_m - R_2)(T_m - T_l) + (\alpha+\beta)(T_m - T_l)^2/2}{(\lambda_m - R_1)(\lambda_m - R_2)} \tag{15}$$

$$E[\tau_3|2] = \frac{(\lambda_m - R_1)\gamma_2 + (\lambda_m - R_1 - \alpha\gamma_2)(T_m - T_l) - (\alpha+\beta)(T_m - T_l)^2/2}{(\lambda_m - R_1)(\lambda_m - R_2)} \tag{16}$$

Example: We choose the following parameters for the two-states Markov chain:

$$\alpha = \beta = 0.2s^{-1} \text{ and}$$

$$R_1 = 0.7\ Mbs\ ,\quad R_2 = 1.3\ Mbs$$

These parameters correspond to a video sequence containing low and high motion of equal amount and each low or high period last for 5 seconds on the average. The average rate is 1.0 Mbs. We choose the following transmission rates:

$$\lambda_l = 0.5\ Mbs\ ,\quad \lambda_m = 1.0\ Mbs\ ,\quad \lambda_h = 1.5\ Mbs$$

After calculating the mean threshold crossing times, the relative frequency of each rate can also be obtained. Let f_l, f_h and f_m be the proportion of time each rate is used. Obviously,

$$f_l + f_h + f_m = 1 \tag{9}$$

Furthermore, the average rate, R_{av} is given by

$$R_{av} = f_l\lambda_l + f_h\lambda_h + f_m\lambda_m \tag{10}$$

Consider a long period t. Let n_h and n_l respectively be the number of times T_l and T_h are crossed during t . Since each low or high rate period is followed by a period with medium rate $n_l(E[\tau_1] + E[\tau_3]) + n_h(E[\tau_2] + E[\tau_3]) = t$. The average rate over period t is R_{av}, i.e., $n_l(E[\tau_1]\lambda_l + E[\tau_3]\lambda_m) + n_h(E[\tau_2]\lambda_h + E[\tau_3]\lambda_m) = R_{av}t$. Combining the last two equations we have

$$\frac{n_l}{n_h} = \frac{E[\tau_2](\lambda_h - R_{av}) + E[\tau_3](\lambda_m - R_{av})}{E[\tau_1](R_{av} - \lambda_l) + E[\tau_3](R_{av} - \lambda_m)} \tag{11}$$

On the other hand,

$$\frac{f_l}{f_h} = \frac{n_l E[\tau_1]}{n_h E[\tau_2]} \tag{12}$$

We obtain f_l, f_h and f_m by solving equations (9), (10), (11) and (12).

The analysis technique developed in this section is applicable to any Markov chain model. In the following subsection, as an example, we derive the solutions for the mean first passage times in detail for a two-states Markov chain.

3.2. Two-states Markov Chain Model

We model the process describing the rate at which the bits are removed from the receive buffer with a two-states Markov chain. For video encoding schemes that use only interframe technique without motion estimation, two-states model can be applicable. A video sequence containing periods of high and low motion can be modeled by two states, one state with low bit rate (corresponding to low motion) and the other state with high bit rate (corresponding to high motion). Let

$$Q = \begin{bmatrix} -\alpha & \alpha \\ \beta & -\beta \end{bmatrix}$$

be the state transition rate matrix of the Markov chain. $1/\alpha$ and $1/beta$ are matched to average durations of high and low motion periods. Without loss of generality assume that $R_1 < R_2$. The roots $\theta_{1,2}$ of (6) are given by

$$\theta_1(\lambda) = \frac{\beta(\lambda - R_1) + \alpha(\lambda - R_2)}{(\lambda - R_1)(\lambda - R_2)}\ , \quad \theta_2(\lambda) = 0$$

The high rate λ_h is chosen to be larger than both R_1 and R_2 in order to have a drift towards T_m after hitting T_l, whereas the low rate λ_l is similarly selected smaller than both R_1 and R_2. The medium rate λ_m is chosen as the average rate, $\lambda_m = (R_1\beta + R_2\alpha)/(\alpha + \beta)$. Hence we have

$$\lambda_l < R_1 < \lambda_m < R_2 < \lambda_h$$

and define the N-dimensional vector

$$\underline{F}(\theta) = [F_1(\theta), \ldots, F_N(\theta)]^T \tag{4}$$

where N is the number of states in the Markov chain. We prove in Appendix A that $\underline{F}(\theta)$ can be written as

$$\underline{F}(\theta) = (Q + \theta D)^{-1} \underline{b}(\theta) \tag{5}$$

where $D = diag\{\lambda - R_s\}$ is the drift matrix and $\underline{b}(\theta)$ as defined in Appendix A is an N-dimensional vector. With the rate control process, the probability of buffer overflow and underflow will be very small and hence the boundary conditions at 0 and B_M are neglected in the analysis.

The inverse Laplace transform can be performed by using partial fraction expansion. As shown in Appendix A (equations (21) and (22)) we can write

$$\underline{b}(\theta) = e^{-\theta B_1} \underline{b}_1 + e^{-\theta B_2} \underline{b}_2$$

where $\underline{b}_1$ and $\underline{b}_2$ are obtained by applying boundary conditions at B_1 and B_2. Let $\{\theta_k\}_{k=1}^N$ be the roots of the equation

$$det(Q + \theta D) = 0 \tag{6}$$

Since all row sums of Q are zero, $\theta = 0$ is a root of (6), say $\theta_N = 0$. We observe that both $\underline{b}_1$ and $\underline{b}_2$ contain the factor $1/\theta$. If all the roots of (6) are distinct, we write

$$\underline{F}(\theta) = \left[\sum_{k=1}^{N-1} \frac{\underline{A}_k}{\theta - \theta_k} + \frac{\underline{A}_N}{\theta^2} + \frac{\underline{A}_{N+1}}{\theta} \right] e^{-\theta B_1} + \left[\sum_{k=1}^{N-1} \frac{\underline{B}_k}{\theta - \theta_k} + \frac{\underline{B}_N}{\theta^2} + \frac{\underline{B}_{N+1}}{\theta} \right] e^{-\theta B_2} \tag{7}$$

where

$$\underline{A}_k = \lim_{\theta \to \theta_k} (\theta - \theta_k)(Q + \theta D)^{-1} \underline{b}_1$$

$$\underline{A}_N = \lim_{\theta \to 0} \theta^2 (Q + \theta D)^{-1} \underline{b}_1$$

$$\underline{A}_{N+1} = \lim_{\theta \to 0} \frac{\partial}{\partial \theta} \left(\theta^2 (Q + \theta D)^{-1} \right) \underline{b}_1$$

and $\{\underline{B}_k\}_{k=1}^{N+1}$ are similarly defined with $\underline{b}_1$ replaced by $\underline{b}_2$. If there are repeated roots of (6), the partial fraction expansion can be obtained accordingly.

Since we are interested in the inverse Laplace transform within the region $B_1 \leq x \leq B_2$, we perform the operation for only the first term in (7). The application of the boundary conditions in obtaining $\underline{b}_1$ and $\underline{b}_2$ nullifies the solution outside $B_1 \leq x \leq B_2$. Let $\underline{H}(x) = [E[\tau|1, x], \ldots, E[\tau|N, x]]^T$ be the inverse Laplace transform of $\underline{F}(\theta)$. We have for $B_1 \leq x \leq B_2$

$$\underline{H}(x) = \sum_{k=1}^{N-1} \underline{A}_k e^{\theta_k (x - B_1)} + \underline{A}_N \frac{(x - B_1)^2}{2} + \underline{A}_{N+1}(x - B_1) \tag{8}$$

The complexity of the main computations in obtaining $\underline{H}(x)$ is in the order of N^3 by the standard Gaussian elimination for the solutions of $\underline{b}_1$ and $\underline{b}_2$.

3.1. First Passage Time Analysis

We analyze the expected time between threshold crossings. We assume that the feedback information is immediately available at the server. For local area networks propagation delay will be small compared to the mean period between rate changes and thus can be neglected.

We define three different first passage times:

- τ_1 = First passage time from T_h to T_m (corresponding to state transition $L \rightarrow M$).
- τ_2 = First passage time from T_l to T_m (corresponding to state transition $H \rightarrow M$).
- τ_3 = First passage time from T_m to either T_h or T_l (corresponding to state transitions $M \rightarrow L$ or $M \rightarrow H$ respectively).

In order to find the mean values of τ_1, τ_2 and τ_3, we define the following first passage time:

$$\tau = \min\{t : x(t) = B_1 \text{ or } x(t) = B_2 \text{ with } x(0) = x, S(t) = s, \text{ arrival rate } \lambda, B_1 < B_2\}$$

where $x(t)$ and $S(t)$ denote respectively the length of the buffer and the state of the Markov chain at time t. We define $E[\tau|s,x]$ as the expected value of τ starting at state (s,x). $E[\tau_i|s]$, $i = 1,2,3$ can be computed from $E[\tau|s,x]$ as follows:

- $E[\tau_1|s] = E[\tau|s,T_h]$ with $B_1 = T_m$, $B_2 = \infty$ and $\lambda = \lambda_l$.
- $E[\tau_2|s] = E[\tau|s,T_l]$ with $B_1 = -\infty$, $B_2 = T_m$ and $\lambda = \lambda_h$.
- $E[\tau_3|s] = E[\tau|s,T_m]$ with $B_1 = T_l$, $B_2 = T_h$ and $\lambda = \lambda_m$.

$E[\tau|s,x] = 0$ for $x \geq B_2$ and $x \leq B_1$. For $B_1 < x < B_2$ and starting at a state s with $\lambda > R_s$, the queue length will hit the upper threshold B_2 if the Markov chain stays at s for longer than $(B_2 - x)/(\lambda - R_s)$. If the state changes earlier, $E[\tau|s,x]$ can be written recursively:

$$E[\tau|s,x] = e^{-q_s \frac{B_2-x}{\lambda-R_s}} \frac{B_2 - x}{\lambda - R_s} + \sum_{s' \neq s} q_{ss'} \int_0^{\frac{B_2-x}{\lambda-R_s}} e^{-q_s t}[t + E[\tau|s', x + (\lambda - R_s)t]]dt \qquad (1)$$

where $q_{ss'}$ is the transition rate from s to s' and $q_s = \sum_{s' \neq s} q_{ss'}$ is the rate of the exponential distribution governing the time spent at s.

When the chain starts at a state s with $\lambda < R_s$, the buffer length will hit the lower threshold B_1 if no transition occurs from s for a duration of at least $(x - B_1)/(R_s - \lambda)$ and otherwise $E[\tau|s,x]$ can be written recursively:

$$E[\tau|s,x] = e^{-q_s \frac{x-B_1}{R_s-\lambda}} \frac{x - B_1}{R_s - \lambda} + \sum_{s' \neq s} q_{ss'} \int_0^{\frac{x-B_1}{R_s-\lambda}} e^{-q_s t}[t + E[\tau|s', x + (\lambda - R_s)t]]dt \qquad (2)$$

We define the Laplace transform $F_s(\theta)$ of $E[\tau|s,x]$ with respect to the initial buffer length as

$$F_s(\theta) = \int_0^{\infty} E[\tau|s,x]e^{-\theta x}dx \qquad (3)$$

change the rate of the multimedia flow to prevent buffer overflow and underflow. All possible threshold crossings are given in Figure 4, each transition labeled from 1 to 4, where each number corresponds to the state transition of the server transmission process to the new rate. The buffer thus is driven by a state dependent arrival process.

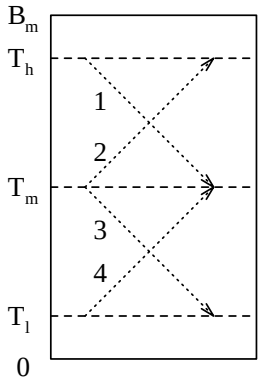

Figure 4: Threshold crossings at the receive buffer

The rate at which user removes bits from the buffer is modeled by a fluid flow process modulated by a continuous time Markov chain with state transition rate matrix Q. When the chain is in state s, information is removed at a rate R_s (in bits per second) from the buffer. The Markov chain model captures the time correlation of rate processes generated by many multimedia sources such as VBR video encoders. The Markov chain model of a rate process can be obtained by using the statistics of the process both in time and frequency domains. By looking the histogram of the rate process showing the frequency of each rate, one can identify clusters and assign a state to each cluster with the rate of the state equal to average rate of the cluster. The relative frequency of each cluster gives the steady state probability of the corresponding state. The time behavior of the rate process can be used to obtain which transitions between clusters are possible. The average time rate stays within a cluster gives the sum of the transition rates out of the corresponding state. The Markov modulated fluid flow model has been widely used to model the cell arrival process in ATM networks since its introduction[11].

In multimedia applications, user may remove data from the buffer in batches at discrete times. As an example, an MPEG video decoder extracts each frame individually. However, if the thresholds are well separated, the time between threshold crossings will be much larger than the time between frame removals. For the computation of mean threshold crossing times, it is unnecessary to concentrate on the detailed behavior of frames. In the larger time scale the bits are as if being removed continuously. Thus, fluid flow model applies for the analysis of the events occurring in this time scale.

The following analysis can be incorporated into the client rate control protocol that adaptively changes the system parameters to achieve the desired performance during the course of a service. The client uses a Markov chain model to characterize the rate process. The parameters of the model can be updated by monitoring the rate process through a time window up to present. The buffer thresholds and transmission rates to attain a satisfying performance can be obtained by using the analysis and new transmission rates are sent back to the server.

the average rate, and very often they are assigned to be a certain factor of the average rate. To safeguard against errors in estimating the peak and lowest rate, overflow or underflow conditions may be used to adjust these rates. For example, an overflow may temporarily result in a requested reduction of transmit rate to 0. Repeated overflow may necessitate a decrease of λ_l. Repeated underflow may necessitate an increase of λ_h.

In the following sections, theoretical and experimental statistics are obtained for the resulting traffic processes and buffer occupancy.

3. Analysis of the rate control process

In this section we analyze the performance of the large receive buffer. In particular we derive the mean duration between threshold crossings by using a first passage time analysis. The frequency of the rate change requests by the client to the server determines the amount of signalling required by the rate control protocol. The fraction of time the server is transmitting at each rate is also computed. Finally, a numerical example is presented for a two-states Markov chain model of the client decoding algorithm for VBR video service.

The choice of the three buffer thresholds as well as the transmission rates determine the frequency of rate change requests to maintain satisfactory performance for the multimedia service. For a fixed buffer size, if the thresholds are chosen at large distances from each other, the amount of signalling will be low at the expense of high overflow and underflow probability. The statistics of the rates used by the client decoding algorithm is another factor in selecting the thresholds. For example for a VBR video application containing long periods of high and/or slow motion, the thresholds should be closer to prevent frequent buffer overflow and/or underflow. On the other hand for a video sequence having bursts of high motion, closer thresholds will cause unnecessary amount of signalling.

In the following analysis the multimedia arrival process is modeled as a fluid flow generated by a finite-state machine (FSM) having three states: Low(L), Medium(M) and High(H). When the FSM is in state L, M or H the arriving bit stream is a constant rate fluid flow with rate λ_l, λ_m or λ_h respectively with $\lambda_l < \lambda_m < \lambda_h$. The state transition diagram of the FSM is given in Figure 3 with each state transition labeled from 1 to 4.

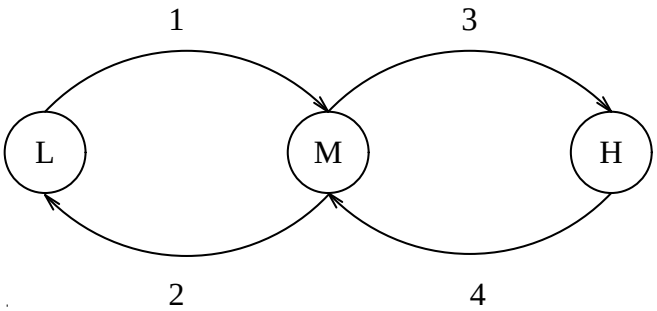

Figure 3: FSM model for the transmission rate process

The client buffer has size B_M and has three thresholds: T_l, T_m and T_h with $T_l < T_m < T_h$. These thresholds are used by the client to produce feedback information to the server asking to

engineering requires certain knowledge of traffic statistics.

The second kind of control, which is the focus of this paper, consists of feedback control, namely that the downstream buffer occupancy determines the rates of the valves. For example, a high occupancy of the receive buffer indicates that the transmit rate is too high compared to the video display bit rate. This low display rate could result from an inherently low video coding rate or the failure of the client to decode at the regular frame rate. The client then sends a feedback request to the server for a reduction in the transmit rate. Similarly, a low occupancy of the receive buffer may result in a feedback request from the client to the server for an increase in the transmit rate. However, a low occupancy of the receive buffer can also result from a congested network, with data accumulating in the network buffer. In this circumstance, increasing the transmit rate would be detrimental. This condition should be detected by a mismatch between the requested transmit rate and the receive rate. Congestion is then alleviated by measures such as lowering the frame rate for the video and subsequently the transmit rate.

The advantages of feedback control are many. First, this protocol emphasizes client QoS control, taking into account that the receiver has better and immediate knowledge of the condition of the end-to-end connection, including the network condition which may not be readily accessible to the transmitter. In certain sense, the effect of all upstream congestion due to the server or the network is detected, differentiated, and alleviated by the action of the client. Second, the transmitter need not examine the timing relationship and data format of the media, thus reducing the computational load of the server which often serves tens and possibly hundreds of connections at the same time. Third, the feedback automatically takes care of client-server synchronization. Fourth, this feedback mechanism does not require a detailed description of the video coding rate process other than the mean rate and hence it is robust to errors in traffic models. If a large buffer is used, the frequency of feedback actions is low, albeit at the expense of a large delay. This infrequent change of a constant requested rate allows careful and infrequent bandwidth reservation[2]. Substantial traffic averaging is achieved as a result. Hence feedback control is more suitable for retrieval of stored media, for which a larger delay between the transmitter and the receiver is allowed.

Thresholds are set for the server cache, the network buffer, and the client buffer. For the server cache, a cache request to the hard disk is generated when the cache occupancy is lest than half full. The cache manager then schedules a disk read to fill up the emptied half of the cache. To detect the occupancy level of the network buffer, the client keeps track of the receiver deficit as an accumulation of the difference between the requested transmit rate and the received rate. If this deficit exceeds a certain threshold, we declare the network throughput as a bottleneck and actions will be taken to reduce the frame rate for the session. Thus the client interface adjusts the media quality adaptively with respect to the transport capability of the underlying network. The receive buffer occupancy is used as control information for maintaining client-server synchronization. There are three buffer thresholds T_h , T_m , T_l, namely the high, medium, and low thresholds. When the buffer occupancy crosses any one of these thresholds, a new transmit rate λ_h , λ_m , λ_l is requested if that rate is not the current transmission rate. The medium rate λ_m is equal to the average rate of the media, which is easily found by dividing the size of the media file by the duration of the media display. The high threshold should normally be higher than the peak rate, and the low threshold should normally be lower the the lowest rate. These extremal rates are more difficult to obtain than

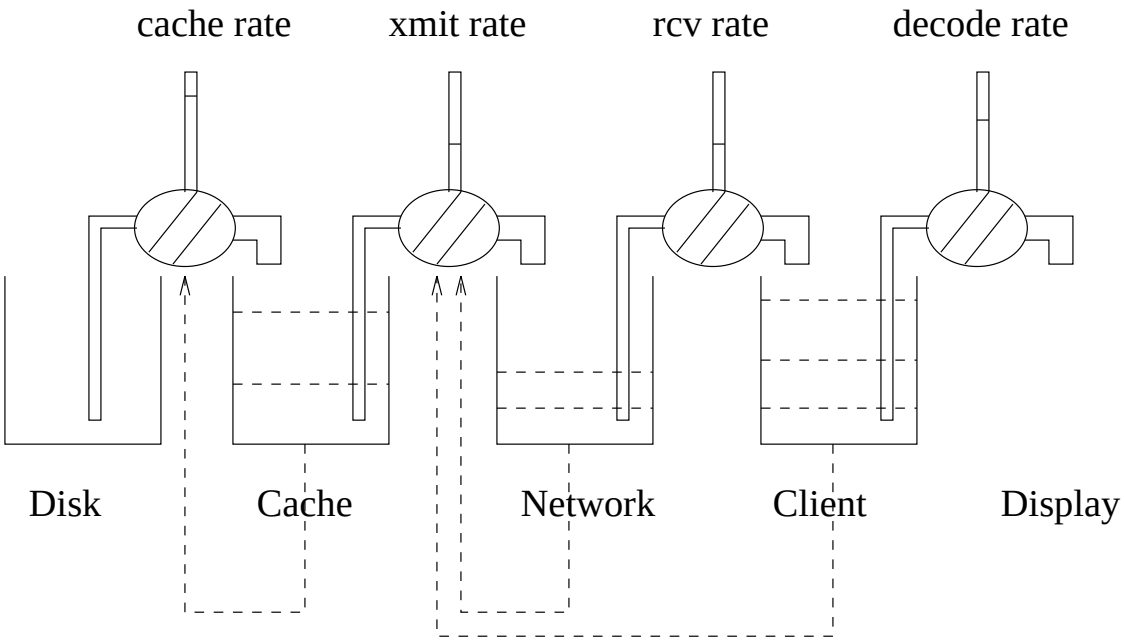

Figure 2: Client-based rate and QoS control

Connecting these buffers are variable rate valves, some of which could be controlled using the state information of one or more of the previously described buffers. For stored video retrieval, the transfer rate from the hard disk to the system cache is dictated by the constant retrieval speed of the bus of the hard drive, even though the media stream may be of variable rate. For teleconferencing, the transfer rate could be highly variable as a function of the type of video frame (I,P, and B frames for MPEG[4]) as well as the amount of motion and the granularity of the video. Some rate smoothing is necessary via the use of the transmit buffer. The transmit valve is probably the most critical control in the pipeline, performing the vital traffic shaping function. The receive valve on the client end ideally should receive information at the same rate as the transmit valve plus a small transit latency. The receive rate may match the transmit rate closely by adequate congestion control methods such as by allocating buffer and bandwidth resources[2] within the network. The video display valve empties data from the client buffer at a rate to maintain a smooth play back.

Transmitter-receiver synchronization is achieved through flow rate modulation. The control of rates as a function of buffer occupancy can be of two kinds. The first kind, which receives more attention in the literature [8][9], consists of feedforward control, namely that the upstream buffer occupancy determines the rates of the valves downstream. For example, a high occupancy of the transmit buffer may result in a feedforward increase in the transmit rate and the display rate. A high transmit buffer occupancy could result from a surge in the media coding rate, such as that resulting from motion in the video.

Feedforward control is often used for teleconferencing for which delay should be less than tens of milliseconds. Subsequently, the buffers in the end-to-end connection should be small. As a result, control actions may be frequent. Such frequent adjustments within the network could be difficult to achieve and often bandwidth overengineering is used to minimize that effect of rate surges. Such

We believe that delay is a significant measure of the Quality of Service for multimedia. Here, we distinguish between two kinds of delay, latency versus jitter. Latency, defined for video, audio, and image transport, is the delay between signal generation (or retrieval) and signal display. Jitter, defined for continuous media streams such as audio and video, results from the disruption of the media as a consequence of underflow or overflow conditions (Figure 1). The underflow jitter rate is defined as the fraction of time the received stream is paused due to underflowing. The overflow jitter rate is defined as the fraction of time the received stream is lost due to overflowing. The sum of these two rates is termed the jitter rate, which measures the degree of jitterness in the media stream. This jitterness is due largely to the failure to synchronize the server and the client in order to maintain continuous flow. Such synchronization is achieved through buffer occupancy feedback in this paper.

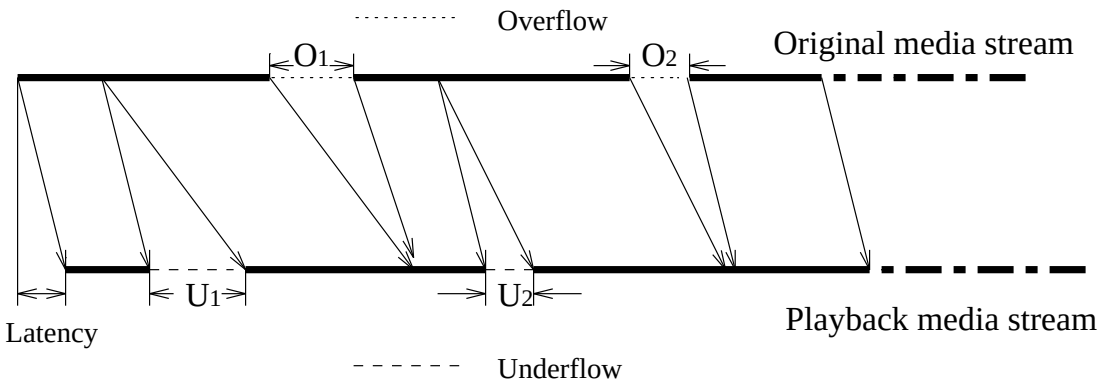

$$Overflow\ jitter\ rate = \frac{\sum_i O_i}{T}$$

$$Underflow\ jitter\ rate = \frac{\sum_i U_i}{T}$$

Figure 1: Jitter rate related to underflow and overflow

2. A feedback flow control and synchronization paradigm

In the GRAMS implementation, the media stream from the server to the client may be modeled as fluid flow through a number of valves and buffers as shown in figure 2.

There are essentially 4 buffers where the media stream may reside. First, the media stream may be stored in a hard disk. For teleconferencing, the media stream may be generated by the capture board, and subsequently compressed by media coding algorithms. Second, these streams are then cached at the transmit buffer. Third, the network, due to its transit latency and buffers within the network, may be viewed as another buffer. Fourth, the receive end may buffer a sufficient amount of the media stream for the purposes of maintaining a continuous stream for display and suitable synchronization with the transmit end.

Client-Server Synchronization and Buffering for Variable Rate Multimedia Retrievals

Joseph Y. Hui, Ezhan Karasan, Jun Li, Julio Navas, Junbiao Zhang

ABSTRACT

We consider the use of large buffers and feedback as a mechanism to maintain loosely coupled synchronization between a multimedia server and a client. The multimedia stream is modeled as a fluid flow through rate controlled valves and buffers with multiple thresholds. These thresholds are used to control the rates upstream. We employ a fluid flow and first passage time analysis to understand the traffic process through the pipelines and the buffers. This feedback mechanism is implemented in GRAMS, an adaptive multimedia client-server system. Experimental statistics are gathered for the purpose of traffic engineering.

1. Introduction - Issues of synchronization and buffering for multimedia

Synchronization, rate control, and buffer management between the source and the destination[6][12][7] are three closely related problems to be solved in order to provide satisfactory quality of service for multimedia communication. In this paper, we shall devise feedback control mechanisms for these three problems, analyze the stochastic behavior of the resulting problem of fluid flow with feedback, and give empirical traffic data from the resulting implementation.

Multimedia communications, as the name implies, involve media of different types such as video, audio, images, text, and data. These communication sessions could be further classified according to their requirements for synchronization and delay. First, real-time communications such as teleconferencing require the strictest synchronization and the least time differences among the time instants of signal capturing, signal coding, signal buffering, signal transmission, signal reception, and signal display. The end-to-end delay typically should normally be less than tens of millisecond. Second, retrieval of multimedia information requires only the display of the audio-video at the same rate as its capturing. The delay between signal retrieval and signal display could be as large as several seconds. However, larger delay may result in unsatisfactory response time for the client. Also, a large delay may require the use of a large buffer somewhere between the server and the client display. Third, image transport imposes almost no synchronization requirement among the components of the signal since the image typically is displayed upon the completion of the entire image transmission. The delay of concern here is the delay between the initiation of an image request, till the complete image is received. This delay ideally should be less than a second, but delay less than ten millisecond may be of no subjective advantage to the client.